

Capillary Sensors with UV-Forced Degradation and Fluorescence Reading of Chemical Stability and Polycyclic Aromatic Hydrocarbons Presence in Diesel Fuels

Michał Borecki

Institute of Microelectronics and Optoelectronics
Warsaw University of Technology
Warsaw, Poland
e-mail: borecki@imio.pw.edu.pl

Michael L Korwin -Pawlowski

Département d'informatique et d'ingénierie
Université du Québec en Outaouais
Gatineau, Québec, Canada
email: michael.korwin-pawlowski@uqo.ca

Mateusz Gęca

Institute of Microelectronics and Optoelectronics
Warsaw University of Technology
Warsaw, Poland
e-mail: mati.geca@gmail.com

Przemysław Prus

Blue Oak Inventions
Wrocław, Poland
email: pprus@boinv.com

Jan Szmidt

Institute of Microelectronics and Optoelectronics
Warsaw University of Technology
Warsaw, Poland
e-mail: j.szmidt@imio.pw.edu.pl

Abstract - There are many standards and types of laboratory equipment for examination of specific properties of diesel fuels. The basic standards of diesel fuel stability require examination taking a relatively long time, counted in days. The development of new methods of diesel fuel stability testing has as its aim accelerated ageing of the examined samples. The most popular of accelerated ageing factors are the increase of temperature and oxidation. In this paper a new method with diesel fuel sample positioned in a capillary and ultraviolet radiation used as degradation factor is proposed. Two possible optical sensor configurations are described as well as the data analysis method for classification of premium and standard commercial diesel samples. The comparison of two sensor configurations was made with the same fuel samples which included winter and summer premium diesel fuel as well as eco winter diesel fuel, unmodified and modified with sludge protection additive. The results of sensor analysis during fuel examination prove that 40 minutes of UV degradation and sequential fluorescence reading at 10 selected moments of time coupled with data processing is enough to evaluate diesel fuel chemical stability and quality. In the experiments light of 265nm and 365nm wavelengths was used correspondingly for degradation and fluorescence reading. We found that chemical stability of fuels was related to the amplitude variations of characteristic emitted fluorescence signals. The concentration of polycyclic aromatic hydrocarbons in fuels was related to the amplitude of signals emitted from excited samples. The UV examination indicated that fuel's chemical stability was better observable with forced degradation and excitation at 265nm, while fuel's polycyclic aromatic hydrocarbons presence was better observable with excitation at 365nm.

Keywords-diesel fuel; fuel quality; fuel stability; PAHs detection, capillary sensor; fluorescence sensor; UV fuel degradation.

I. INTRODUCTION

This paper's focus is on selected aspects of a sensor using a capillary optrode and UV radiation as the fluorescence excitation factor and fuel degradation initiator that enables rapid testing of chemical diesel and biodiesel fuels stability. The principle and preliminary results of this work were presented in [1].

A. Diesel and biodiesel fuel –as seen from the user's and producer's sides

On the diesel fuel user's side low cost and high quality of the fuel are important. Diesel fuel quality is analyzed with reference to diesel engine operating characteristics, such as starting ease, low noise, low wear, long life, sufficient power, low temperature operability, and low emissions [2].

On the fuel producer's side, the quality of diesel fuel is determined by quality standards. These quality standards differ for diesel and biodiesel fuels. The most popular standards of diesel fuels are ASTM D 975 introduced by the American Society for Testing and Materials and EN 590 introduced by the European Committee for Standardization. Respectively, the standards for biodiesel fuels are the ASTM D 6751 in the USA and the EN 14214 in Europe. In this approach, the quality of fuel can be described as a set of laboratory measured fuel parameters, like for example: the

cetane number, pour point, viscosity, density, acid number, the result of accelerated oxidation stability test, and result of test for gum content in fuels by jet evaporation, as well as sulfur, nitrogen and oxygen contents of fuel composition.

The common feature of fuel user's and producer's sets of fuel quality parameters is that they depends on diesel fuel composition, which changes in storage due to presence of some chemical active fuel components [3].

B. Type and composition of diesel and biodiesel fuels

The diesel and biodiesel fuel consists of the fuel base, the fuel improvers and impurities. The type of diesel fuel may be described by the fuel base origin or the technological process.

Petroleum diesel (petrodiesel) is the fuel produced in a refinery as a blend of straight-run product, fluid catalytic cracking light cycle oil, and hydrocracked oil. The straight-run product may be acceptable as diesel fuel. Synthetic diesel (syndiesel) can be produced from any carbonaceous material. The raw material is gasified and after purification is converted in the Fischer-Tropsch process. The synthetic diesel generally is the first class fuel base. Fatty-acid methyl ester (FAME), obtained from vegetable oil or animal fats which have been transesterified with methanol is a common biodiesel fuel base composition. FAME has lower oxidation stability than petrodiesel, and it offers favorable conditions for bacterial growth. Hydrogenated oils (HVO) may be produced from the triglycerides from vegetable oil and animal fats. The HVO is a composition of alkanes obtained in the refining and hydrogenation process. Therefore, HVO composition is similar to synthetic diesel like fuel.

Modern petroleum-derived diesel fuel base is composed of about 74% saturated hydrocarbons - primarily alkanes, 25% aromatic and acyclic unsaturated hydrocarbons. The typical chemical formula for diesel fuel base molecule composition is $C_{12}H_{23}$, but the number of carbons in the molecule ranges approximately from C10 to C22. Now, it is worth noting here, that at 25°C alkanes ranging from C5 to C17 are liquids, while alkanes ranging above C17 are in solid state. Therefore, it is expected that in the diesel fuel some solid state hydrocarbons particles are present and form some kind of colloid.

The most common saturated hydrocarbon of diesel fuel is dodecane described with the formula $H_3C(CH_2)_{10}CH_3$. Alkanes have the general chemical formula C_nH_{2n+2} . Alkanes are only weakly reactive with ionic substances, but all alkanes react with oxygen in a combustion reaction [4].

Saturated cyclic liquid hydrocarbons are not alkanes, but they are often called cycloalkanes as are characterized with similar chemical properties as alkanes.

Unsaturated acyclic hydrocarbons fuel content consist primary of alkenes, but alkynes, alkadienes and alkatrienes may be found in diesel fuel.

Acyclic alkenes, with only one double bond and no other functional groups are described by the general formula C_nH_{2n} . It can be seen that for the same number of carbon atoms acyclic alkenes have two hydrogen atoms less than the corresponding alkane. Acyclic alkyne is an unsaturated hydrocarbon containing at least one carbon-carbon triple

bond. The general chemical formula of basic alkyne is C_nH_{2n-2} .

Alkadienes are acyclic hydrocarbons having two carbon-carbon double bonds, while alkatrienes are hydrocarbons having three carbon-carbon double bonds. A simple alkadiene is butadiene, which is a gas with the structure $H_2C=CH-CH=CH_2$. This molecule is important in the chemical industry as is used in production of synthetic rubber. A popular acyclic hydrocarbon containing three carbon-carbon double bonds; is 2,4,6-octatriene, which has the structure $H_3C-CH=CH-CH=CH-CH=CH-CH_3$ and a standard name isooctane. It is a liquid and an important component of gasoline used in relatively large proportions to increase the knock resistance of the fuel.

Unsaturated aromatic (cyclic) hydrocarbons are represented by monocyclic benzene (MAH – monocyclic aromatic hydrocarbon) and by polycyclic aromatic hydrocarbons (PAHs). Benzene is a natural liquid constituent of crude oil and is one of the elementary petrochemicals. The simplest PAH having two aromatic rings is naphthalene (white crystalline solid). The three-ring PAHs compounds are anthracene (colorless solid) and phenanthrene (white powder).

PAHs molecules can be found in coal and in tar as well as in crude oil. Therefore, almost every petroleum product contains various PAHs particles [5]. Diesel fuel is expected to contain PAHs particles ranging from three to five ring systems.

Fuels fabricated for diesel engine may contain bio-component that may reach a few percent of fuel volume. The bio-components' presence is significant from fuel technology, affiliation (bio-diesel) and fuel parameters points of view [6]. Important is that bio-components may be of first or second generation [7]. The first generation of bio-diesel components includes fatty acids methyl esters (FAME) that are characterized by the presence of double bonds, while the second generation components base on hydro-treated vegetable oils (HVO) that seem to be mainly carbohydrates with saturated carbon atoms bonding [8].

The modern diesel fuels include also a range of additives, as for example cetane improvers, antioxidants, detergents, corrosion inhibitors, deposit modifiers, lubricity agents, and biocides [9].

The most popular cetane improver is 2-ethyl hexyl nitrate (2-EHN); the minor significant improver is di-tertiary-butyl peroxide (DTBP). DTBP is a peroxide and its chemical formula is $(CH_3)_3COOC(CH_3)_3$. 2-EHN is nitroalkane, which linear formula is $CH_3(CH_2)_3CH(C_2H_5)CH_2ONO_2$. Both substances include oxygen and are reactive.

It was found that hydrocarbons mixture with C10–C18 particle is the optimum range for microbial metabolism [10]. Therefore, in stored diesel fuel some microorganisms are presented. The microorganisms adhere to the tank walls or settle in the fuel-water interface at the bottom of the tank. Possible routes of entry of microorganisms into the fuel can be from the ground by cracks of buried tanks and from the air, during loading operations. Furthermore, organic biocides with different functional active groups and hydrogen peroxide are in use as additives to diesel fuel [11].

C. Diesel fuel degradation during storage process

Hydrocarbons of diesel fuel may degrade as a result of oxygen presence and reaction initiator. Known reaction initiators are light, temperature and catalyst.

The photochemical reactions caused by light are mainly able to affect the physical properties of some of the oil fractions. They are able to alter the emulsion formation and the solubility of the fuel fractions. This is done by inducing reaction between oil components and other molecules, which makes the molecules more polar and water soluble, so creating new compounds with other physical properties [12]. It seems that there major mechanism involved in photo degradation of oil can be classified as direct or indirect photolysis [13]. Direct photolysis takes place when the molecule of interest absorbs energy from light and further degrades. Indirect photolysis occurs when another molecule absorbs the energy from light and reacts to degrade the molecule of interest. The UV radiation also can suppress a number of microorganisms in diesel fuel [14].

The thermal stability of diesel fuels was examined at different temperatures: higher than 150°C and below 150°C [15].

Saturated hydrocarbons common degradation is a result of oxidation. The products of oxidation include aldehydes, ketones, acids and alcohols which can further transform into multi-particle substances that form resins and sediments [16].

The unsaturated hydrocarbons degradation in standard vessel condition may occur as the oxidation and polymerization process. Certain alkenes undergo self-addition reactions in the presence of specific catalysts or energy supply to produce molecules called polymers. The reaction involves double bonds being converted to single bonds as hundreds of molecules bond and form long chains. It is not possible to give an exact formula for a polymer produced by a polymerization reaction because the individual polymer molecules vary in size [17]. Polymers made from alkenes result in a very long-chain alkane. As a result, it has the chemical inertness of alkanes and form solid sediment in fuel.

Chemical oxidation of PAHs occurs readily, for example, anthracene ($C_{14}H_{10}$) oxidation gives anthraquinone, ($C_{14}H_8O_2$). PAHs react also with singlet oxygen - a high-energy form of oxygen. PAHs react with acetone in photo degradation. For example, naphthalene with 1% acetone mixture during UV irradiation results in 1,2-Benzenedicarboxaldehyde generation. The examination at 254, 310 and 365 nm, wavelength shows that the influence of wavelengths on photodegradation rates of PAHs was significant [18]. The irradiation at 365nm found to be effective in oxidation of PAHs. For example, naphthalene $C_{10}H_8$ intermediates produced during UV irradiation in oxygen presence are:

- $C_8H_6O_2$ - 1,2-Benzenedicarboxaldehyde,
- $C_9H_6O_2$ - 2H-1-benzopyran-2-one,
- $C_{10}H_6O_2$ - 1,4-Naphthalenedione,
- $C_{10}H_8O$ - 1-Naphthalenol,
- $C_{10}H_6O_3$ - 2-Hydroxy-1,4-naphthalenedione, [19].

Cetane improvers decompose rapidly and form free radicals when exposed to temperatures above 100°C. These radicals increase the rate of main fuel components decomposition; therefore, the ignition delay is negatively affected [20].

DTBP molecule during decomposition supplies both the oxidizer and the fuel particles. Thus, it can be used as a fuel in engines where oxygen is limited [21].

2-EHN in liquid phase can decompose in the absence of air as, for example, when pressure and temperature in storage tank increase above 75°C [22]. But, in another report [23], authors suggest that at temperatures below 100°C the decomposition of 2-EHN in diesel fuel is extremely slow, as at 120°C the half-life is 522.7 h. Moreover, in the mentioned paper, the 2-EHN at the 146.3°C and 2400 bar half-life is 88.5 h, while half-life at 1 bar is 16 h. The initial step of 2-EHN particle decomposition is the separation of NO_2 and the rather unstable 2-ethylhexyloxy radical (2-EHO). Thus, we conclude that 2-EHN behavior in diesel fuel environment may depend on fuel composition. Moreover, such conclusion is supported by proposed method of 2-EHN concentration examination in diesel fuel with UV fluorescence examination reported in [24].

The antioxidant additive of diesel fuel principal function is to inhibit the formation of peroxides. Therefore, as can be seen, antioxidants should react with some cetane improvers as for example DTBP.

D. Sensing methods for diesel fuel quality

There are many methods to measure diesel fuel quality. The standardization process of measurement of diesel fuel parameters is still in progress [25]. Nowadays, the basic idea of fuel characterization is a selective and specific measurement of sequent parameters.

Petro-chemic industry representative recognized a series of fuel parameters measured in laboratory conditions, as for example a cetane number (CN), acid-number, flashpoint, lubricity and oxidation stability. Measurements of the mostly recognized fuel quality parameter called ignition quality of fuel (CN) have to be carried out in the Cooperative Fuel Research Engine (CFR-5) or the Ignition Quality Tester (IQTTM). On the other hand, many fuel parameters depend on fuel composition described by distillation results. The distillation parameters may to be measured using the classic distillation unit, or may be measured with automated distillation process analyzer [26]. Oxidation stability of fuel standard measurement with rancimat method refers to oils chemical reaction with gas environment [27]. It should be noted that chemical stability of fuel means thermodynamic stability of a chemical system and refers to chemical internal reaction between fuel components, [28] [29]. Therefore, chemical stability of fuel is not the same as oxidation stability. But, some definitions of the chemical stability refers to the tendency of a material to resist change or decomposition in its natural environment when exposed to air, heat, light, pressure, or other natural conditions.

Contrariwise, fuel users expect parameters set that describe diesel fuel operability and that can be measured in situ. Unfortunately, such set of parameters is not full

standardized, but include engine start characteristic, time of fuel life (stability), fuel transfer dynamics from tank to injection unit and fuel contamination.

A set of method for fuel contamination with different chemicals as for example non-transferred vegetable oils, kerosene, PAHs are under development. The examination of bio-components concentration can be made with the use of excitation-emission matrix method for wavelength range of 250-500nm with spectral subtraction fluorescence for range of 300-600nm. This method is precise, but requires expensive equipment [30]. Therefore, mentioned method has been adopted to use with the one light emitted diode as excitation source [31]. But, an investigation result refers only to samples of diesel fuel intentionally contaminated with known concentration of bio-component or kerosene. It is worth noted that time-resolved fluorescence method can be used for classification of the unknown fuels groups as gasoline, diesel, bio-ester and vegetable oil [32]. The fluorescence time delay method and a high pass method are used for the detection of PAHs. In the high pass method, the high pass optical filter was used to remove the scattering of the exciting pulse, as the exciting energy may be too high and destroy detector. For example, naphthalene detection was performed with excitation at wavelength of 266 nm, with 6 ns pulse of 5 mJ, which was repeated at 10 Hz rate [33].

A set of method oriented to examination of oxidation stability of diesel fuels are also under investigations. For example, the method of antioxidant presence in fuel samples with absorption measurement performed at 256 nm has been proposed [34].

Synchronous fluorescence spectroscopy was suggested as a tool to evaluate the photo and thermal degradation results of crude oils [35]. The degradation was performed with sunlight of 350 W/m² that lasts for 100 hours. Oils irradiated showed decreased fluorescence intensity at all wavelengths from 350 to 700nm, when examined in intervals of at least 2 hours.

New methods of diesel fuel fitness-for-use determination that are addressed to implementation in sensors are under development. These methods include measurement of characteristic points of local sample heating of fuel positioned in a capillary [36], measurement of the dynamical rise of fuel in an inclined capillary [37], reading of fluorescence effects in the range of UV-VIS and reading of UV-forced degradation results of closed sample of diesel fuel [38]. Dedicated components of mentioned sensors, as capillary optrodes [39], micro-heaters [40], optoelectronic photodetectors [41] and photodetectors pre-amplifiers [42], have been developed. Also, some aspects of automatization of sensor with capillary set-ups as data filtering and processing [43] as well as influence of man operator are under investigation [44]. Moreover, progress in explored methods of diesel fuel examination is coupled with development of new photonics elements as fluorescent core micro-capillaries [45], improvements in construction of electronic components as electronic modules [46] [47] and improvement in microelectronic manufacturing technology [48].

E. Photo degradation and photo detection possibilities of potentially unstable diesel fuel components

The photo degradation and photo detection of potentially unstable fuels components is possible with radiation that wavelength range is absorbed by fuel in particular by unstable particles.

The maximum absorption of alkenes shifts from deep UV toward longer wavelengths with the increase of the number of carbon-carbon double bonds, for example, H₂C=CH₂ the maximum absorption is at 180nm, for H₂C=CH-CH=CH₂ the maximum absorption is at 217nm, while B-carotene with 11 double carbon-carbon bonds is characterized by the maximum absorption at 455nm [49]. Absorption of UV in oil samples at 230–235 nm allows detection of alkadienes, while absorption at 260, 270 and 280 nm allows detection of alkatrienes [50]. For example, detection of isooctane may be performed as absorbance measuring at 232 nm and 264-272 nm.

Similar dependency of maximum absorption shift can be observed in aromatic unsaturated hydrocarbons. For example, benzene maximum absorption is at 255nm, naphthalene is at 286nm while anthracene is at 363nm. Absorption peaks are also influenced by functional groups while benzene maximum absorption is at 255nm, phenol is at 270nm, and nitrophenol is at 320nm.

PAHs generally absorb light in the 200-400 nm range and strongly fluoresce in 360-430nm range. For example, peak wavelength of excited fluorescence for benzo[a] anthracene is 387nm, for benzo[a]pyrene is 405nm, for benzo[k]fluoranthene is 403nm, for chrysene is 382nm and for phenanthrene is 366nm [51]. It is interesting that the emission spectra of benzo[a]anthracene is characteristic and can be described as hills with two similar peaks with one a little dominant height at 387nm and 410nm and with wavelength symmetric saddle. The naphthalene also has a similar shape with hills peak at 325nm and 335nm. The photo degradation of naphthalene with the addition of nitrogenous air pollutants NO₂ was described [52]. The results indicate that naphthalene degradation occurs when irradiated with UV light > 290 nm. Reaction products were 2-formyl-cinnamaldehyde, 1,4-naphthoquinone, nitronaphthol, o-phthalaldehyde, phthalide and nitronaphthalene. Nitronaphthalene is characterized by unique solvent-dependent fluorescence [53].

Up today, PAHs photo degradation as pyrene and benzo[a]pyrene using ultraviolet sources working at wavelengths of 254, 310 and 365 nm was investigated. The results of UV irradiation intensity on the degradation performance of PAHs show that with the intensity of UV irradiation being increased, the degradation rates of PAHs were higher. Additionally, degradation rates of pyrene were different at different UV irradiation wavelengths [54]. Also, PAHs degradation in real outdoor condition showed a good linear correlation with mean solar radiation intensity [55]. But, it was indicated that photo degradation rates of anthracene, phenanthrene and naphthalene in water surfaces are different. Anthracene half-life was 1 hour, phenanthrene

was 20.4 hours while half-life of naphthalene exceeded 100 hours [56].

F. Intermediate conclusions – selection of UV sources to degradation of unstable fuel components

The diesel fuel is a multicomponent mixture that may be degraded with oxygen, temperature or light irradiation. Classical methods of fuel analysis of oxidation stability require trained chemist, costly equipment and prolonged time of examination or are not precise. On the other hand, fluorescence is a sensitive indicator of photochemical transformations of fuel components [57]. Therefore, examination of chemical stability of diesel fuels may be performed with forced UV degradation and fluorescence reading of signal emitted from unsaturated hydrocarbons.

It should be noted that light absorption in popular PAHs as naphthalene {288 nm}, phenanthrene {252 nm; 275 nm; 294 nm} and anthracene {252 nm; 356 nm} can be addressed with 260 UVTOP LED that emits radiation from 255 nm to 270 nm when calculated for 20% of peak intensity located at 265 nm. This is due fact that aromatic components light absorption characteristics are not narrow peaks of mentioned wavelengths but extends into quite wide bands. For example, naphthalene absorption calculated at half intensity extends from 250nm to 289nm [58].

On the other, hand solar radiation falling to the ground does not include UVC range, but include UVA. The example of intensity of spectral distribution of sun irradiation for sunny day of 09 of May 2018 in Warsaw is presented in Figure 1.

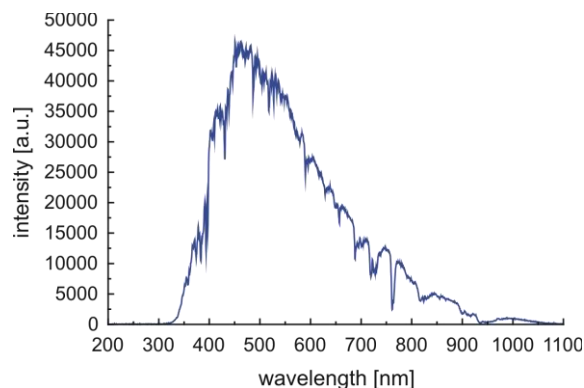


Figure 1. Distribution of intensity of sun irradiation in sunny day of 09 of may 2018 in Warsaw registered at 4pm.

This data may lead to conclusion that radiation of 365nm wavelength is well represented in natural environment. Besides, for such radiation high powers LEDs are available, as for example M365F1.

Therefore, the rest of this paper is organized as follows. Section II describes the sensor construction development including sensor head with optrode as well as optoelectronics system set-up. Section III addresses the results of the analysis fluorescent signal that is recorded during photo degradation at selected wavelength. Section IV goes into conclusions.

II. SENSOR CONFIGURATION

Proposed capillary sensor with UV-forced degradation and fluorescence reading of chemical stability of diesel fuels can be configured with one, two or three UV sources. The UV forced degradation and fluorescence excitation in sensor with one UV source is performed at the same wavelength. The degradation and fluorescence excitation wavelengths can be different in sensor with two or three UV sources. The sensor configuration with a couple UV sources gives possibility to spread wavelengths for degradation and for fluorescence excitation, but the number of combination of measurement configuration increase rapidly with sources number. Therefore, in this paper the configurations of sensors with forced degradation and fluorescence excitation at the same wavelength are examined. The selected wavelengths for sensor examination are 265nm and 365nm. As a UV sources the light emitting diodes are in use correspondingly UVTOP265 LED and M365F1 LED. The examined UV degradation is realized by UV irradiation of sample fuel positioned in capillary for 40 minutes. During this degradation, fluorescence signals are read at 0.5, 1, 5, 10, 15, 20, 25, 30, 35 and 40 minutes.

A. Sensor set-up with one UV source working at 265 nm

The sensor head of the set-up with one UV source working at 265 nm is presented in Figure 2.

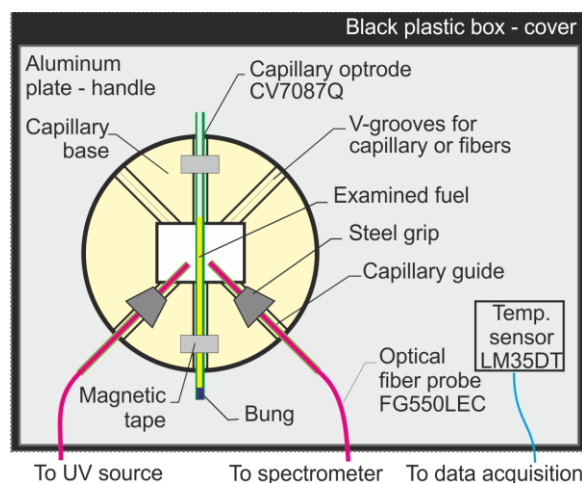


Figure 2. Scheme of the capillary sensor head with one UV source.

The head is coupled to the optoelectronic sensor set-up for UVTOP265 LED according to the scheme presented in Figure 3. The set-up is optically powered by a LED controlled with the hardware D2100 driver that is triggered from a PC with the use of software. The fiber optic divider 1:7 is used to produce a reference signal and to monitor light source parameters with PM100D optical power meter equipped with S120VC photodiode. The head output is connected to Maya 2000pro spectrometer, which is connected to PC and controlled by Ocean Optics software that enables sequential writing of data recorded.

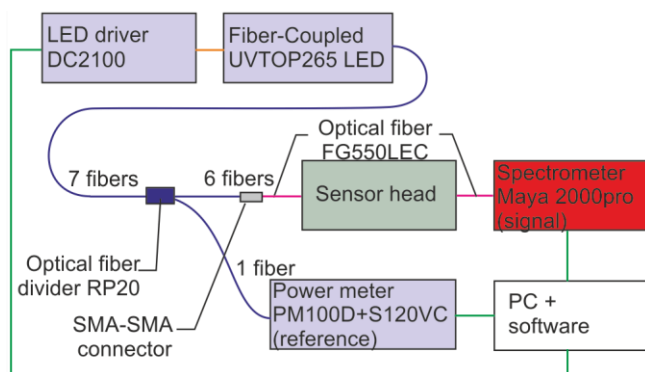


Figure 3. Scheme of the capillary sensor set-up with one UVTOP265 LED.

Data recorded from spectrometer and power meter are processed in each examination for elimination of spectrometer dark signal, light source emitted power drift reduction and for de-noising of signal.

B. Sensor set-up with two UV sources working at 365nm

The sensor set up for head working at 365 nm requires relatively narrow band for fluorescence excitation source as the wavelength of excitation signal is close to emitted band of some PAHs. For example, M365F1 LED bandwidth (FWHM) is 7.5nm and the residual long wavelength radiation may interfere with excited fluorescence signals. Therefore, M365F1 LED using as fluorescence excitation requires optical filtering, which may reduce optical power required for degradation. Thus, dividing optical channel to excitation and degradation leads to the sensor configuration proposed in Figure 4. The head is coupled to the optoelectronic sensor set-up with M365F1 LEDs according to the scheme presented in Figure 5. The sensor set-up for fluorescence excitation and reading with M365F1 LED, contrary to UVTOP265 LED, includes a monochromator adopted as precise optical filter.

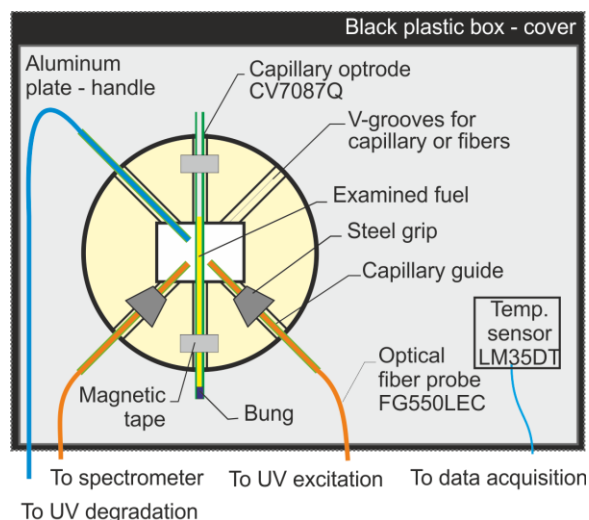


Figure 4. Scheme of the capillary sensor head with two UV sources.

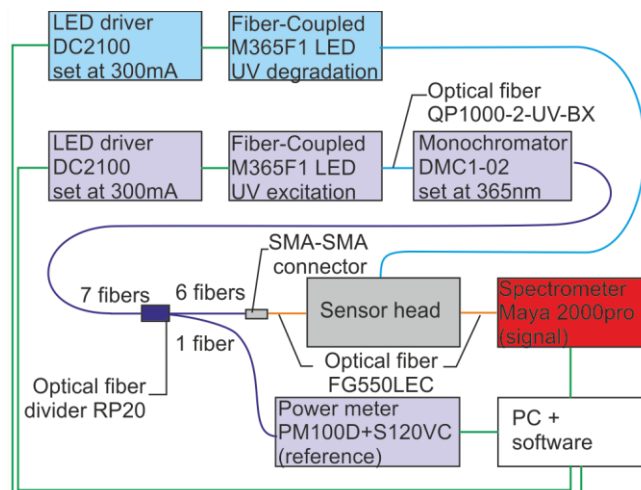


Figure 5. Scheme of the capillary sensor set-up with two UV LEDs.

The utilized monochromator DMC1-02 enables reducing bandwidth to 2nm and fully rejects the long wavelength residual radiation. But this tuning of the M365F1 LED's optical signal to the accuracy required by fluorescence excitation and reading of diesel fuels introduces 1:135 of signal attenuation.

The UV degradation LED working point is set with current stabilization. Therefore, UV power shift can be present and can affect the obtained results. In presented examination, the degradation power was in range from 1293μW up to 1300μW, while the excitation power was in the 8.98μW to 9.34μW range. While fuel oxidation parameters values as induction time, calculated in percent, varies for different fuel type much more than any possible variation of the mentioned LED power.

III. EXPERIMENTAL RESULTS OF FUEL EXAMINATIONS

The six types of diesel fuel (DF) were under examination including three base clear fuels of premium summer type stored for 4 months in dark container in room conditions (PSC), fresh premium winter fuel (PWC) and fresh eco winter fuel (EWC). These fuels catalog data point similar oxidation stability, but eco fuels are expected to contain more PAHs than premium ones. Therefore, for examination purposes, fuels were modified with additional improver intended to be antioxidant and waxes solvent. This way auxiliary fuels names can be written as: premium summer with additional improver (PSA), premium winter with additional improver (PWA) and eco winter with additional improver (EWA). Mentioned acronyms are used in tables that gather experimental data.

The examination was performed for fuel in ambient temperature equal to 22°C±1°C. In such conditions and used measuring procedure include data processing obtained result of examination accuracy is better than 280 [a.u.] while single measurement accuracy is 50 [a.u.] for full scale range equal 64000 [a.u.].

A. Diesel fuels examination with one UV source working at 265nm

The first set of examination was performed in set-up from Figure 3. The family of characteristics for the set of fuels is presented in Figures 6-11.

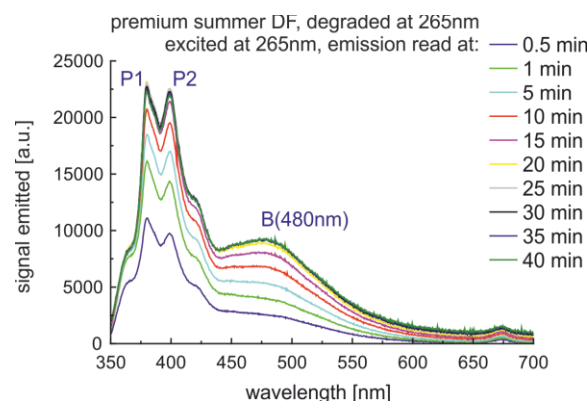


Figure 6. Signal emitted from clear premium summer diesel fuel degraded and excited at 265nm.

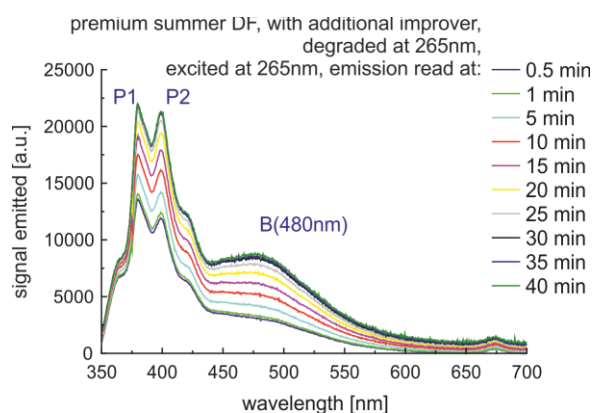


Figure 7. Signal emitted from premium summer diesel fuel with additional improver degraded and excited at 265nm.

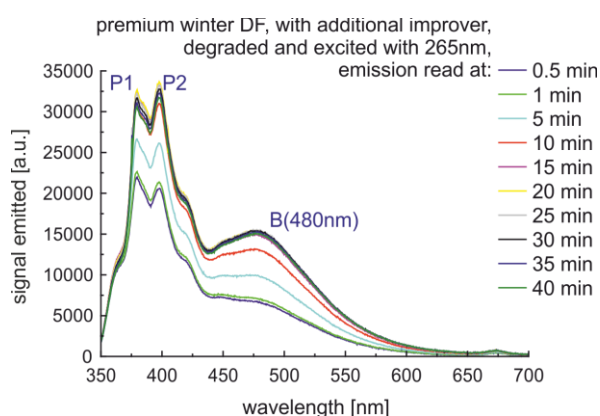


Figure 8. Signal emitted from clear premium winter diesel fuel degraded and excited at 265nm.

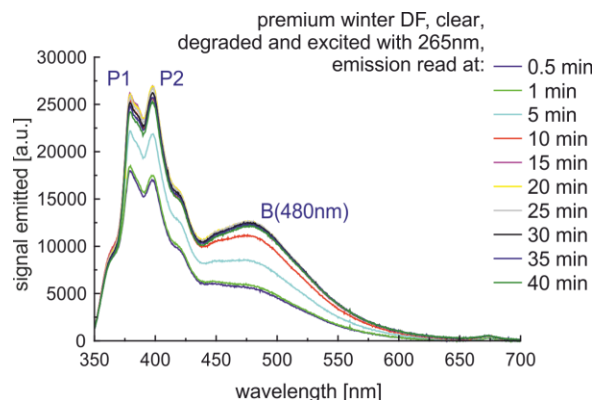


Figure 9. Signal emitted from premium winter diesel fuel with additional improver degraded and excited at 265nm.

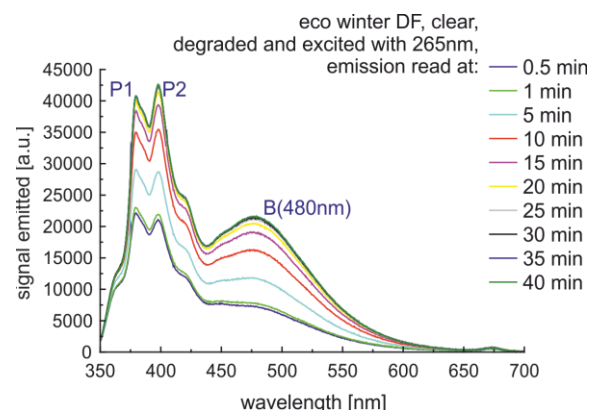


Figure 10. Signal emitted from clear eco winter diesel fuel degraded and excited at 265nm.

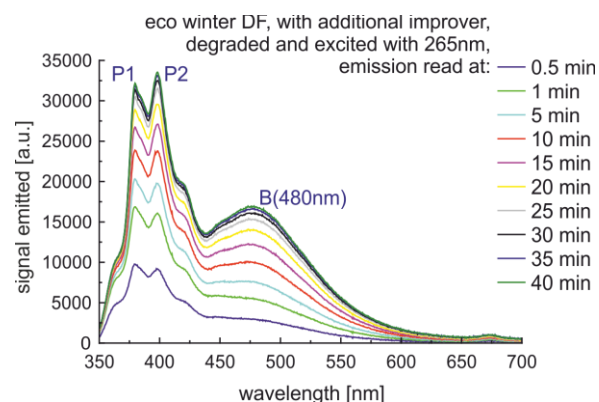


Figure 11. Signal emitted from eco winter diesel fuel with additional improver degraded and excited at 265nm.

The shapes of the characteristics are similar. The characteristic points may be proposed as two peaks P1 at 380nm and P2 at 399nm as well as band signal B480 emitted round 480 nm. For analysis purpose, the characteristics

points P1, P2 and B480 for different fuel types are gathered in Figures 12-14.

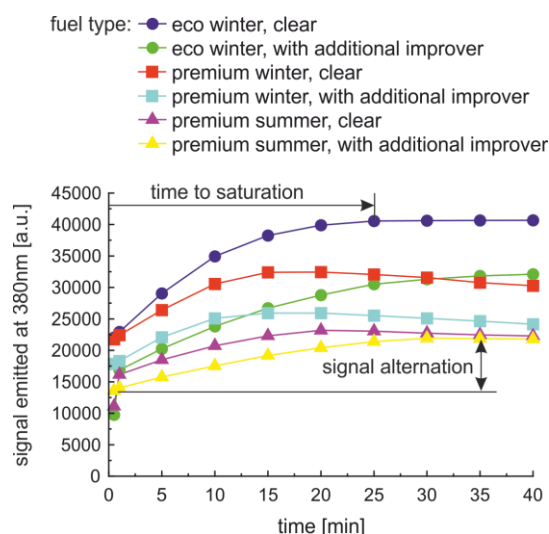


Figure 12. P1 emission at 380nm, excited at 265nm.

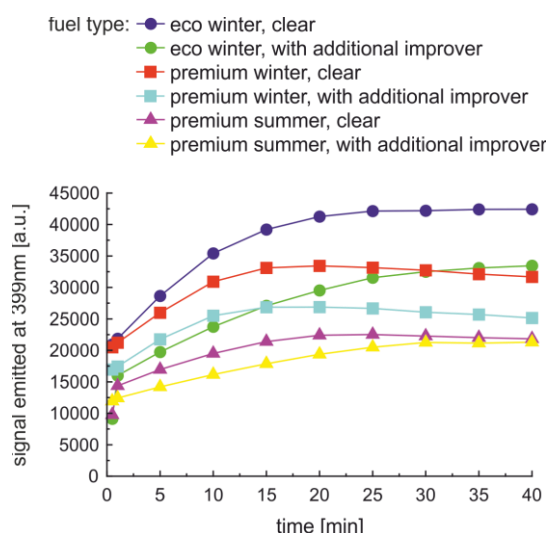


Figure 13. P2 emission at 399nm, excited at 265nm.

The first step of data analysis at Figure 12 should be performed for fuel couples: clear fuel and corresponding fuel with additional improver. In such case the influence of the improver is visible as characteristics shift down with the improver's presence. This shift is not constant, but characteristics pairs are recognizable. The second step of analysis should be performed for fuel types -clear and with additional improver. The clear fuel types characteristics analysis lead to the conclusion that eco fuel generates greater signal at 380nm than premium fuels. But for fuels with improver this statement is not always true.

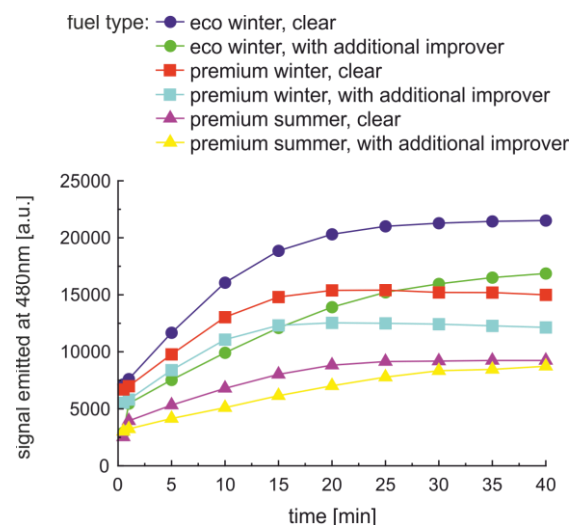


Figure 14. B480 emission at 480nm, excited at 265nm.

The characteristic data points of fuel under with 265nm radiation degradation, counting from the first minute, maximum signal, signal alteration and time to signal saturation at selected wavelength of P1, P2 and B480, are gathered in Table I. The greater is the maximum signal the fuel is expected to contain greater volume of fluorescence particles as PAHs, and therefore be of lower quality. For example, clear eco fuel is described by greater values than the eco fuel with improver, clear premium fuels are characterized by greater values than premium fuels with improver.

TABLE I. DIESEL FUEL EXAMINATION RESULTS WITH ONE UV SOURCE WORKING AT 265NM

| Fuel type | Maximum signal during degradation [a.u.] | | | Signal alteration [a.u.] | | | Time to saturation [min] | | |
|-----------|--|-------|-------|--------------------------|--------------|------------------|--------------------------|----|------|
| | P1 | P2 | B480 | P1max -P1min | P2max -P2min | B480max -B480min | P1 | P2 | B480 |
| EWC | 40676 | 42419 | 21518 | 17733 | 20563 | 13907 | 25 | 35 | 35 |
| EWA | 32101 | 33456 | 16870 | 15236 | 17455 | 11412 | 40 | 40 | 40 |
| PWC | 32448 | 33423 | 15414 | 10021 | 12199 | 8429 | 15 | 20 | 20 |
| PWA | 25929 | 26872 | 12543 | 7626 | 9447 | 6731 | 15 | 20 | 20 |
| PSC | 23181 | 22510 | 9242 | 7031 | 8148 | 5294 | 30 | 25 | 30 |
| PSA | 21925 | 21292 | 8726 | 7891 | 8869 | 5489 | 40 | 40 | 40 |

The signals alternation during degradation can be used for description of fuel stability. Signals changes for all parameters: P1, P2 and B480 indicate that eco fuel changes are greater than for the premium ones. But for premium fuels the signal change dependency on improver addition is not clear. Despite, the expected relation of lower stability of eco fuel compared to premium is confirmed.

Times to saturation value of P1 increase or stay constant when the improver is added to fuel. Similar dependency has been obtained for values of P2 and B480.

B. Diesel fuels examination with two UV sources working at 365nm

Second set of examination was performed in the set-up from Figure 5. The family of characteristics for the set of fuels is presented in Figures 15-20.

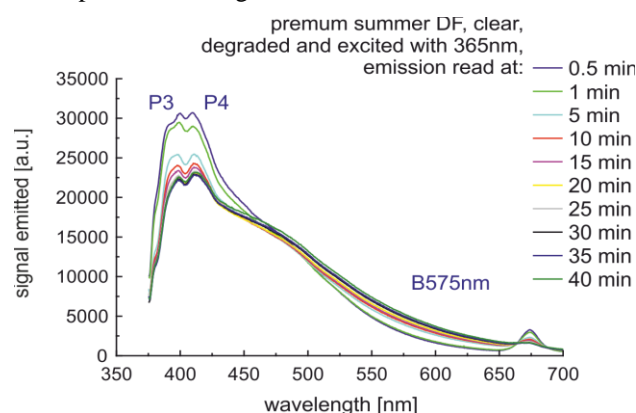


Figure 15. Signal emitted from clear premium summer diesel fuel degraded and excited at 365nm.

The first comparison of characteristics from Figure 15 and Figure 6 shows that peaks are at different wavelength. Therefore the new peaks are numbered as P3 and P4. Moreover, the characteristic changes in B480 bandwidth presented for degradation with 265 nm wavelength now is not observable. Now, the bandwidth of visible changes is from 525nm to 625nm with the greatest variations at about 575nm (B575).

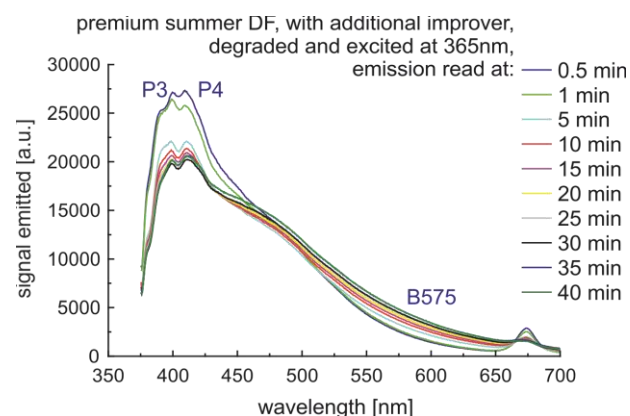


Figure 16. Signal emitted from premium summer diesel fuel with additional improver, degraded and excited at 365nm.

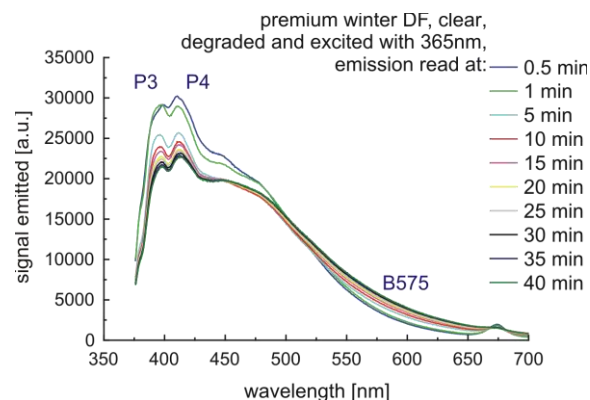


Figure 17. Signal emitted from clear premium winter diesel fuel degraded and excited at 365nm.

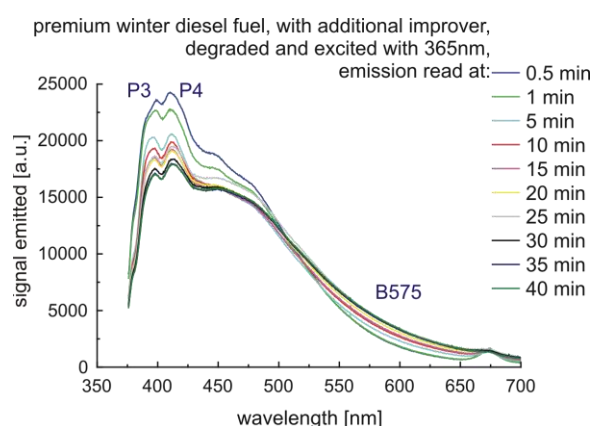


Figure 18. Signal emitted from premium winter diesel fuel with additional improver degraded and excited at 365nm.

Now, the experimental data analysis leads to the conclusion that peak radiation P3 and P4 wavelengths are characterized by minor, but measurable shifts.

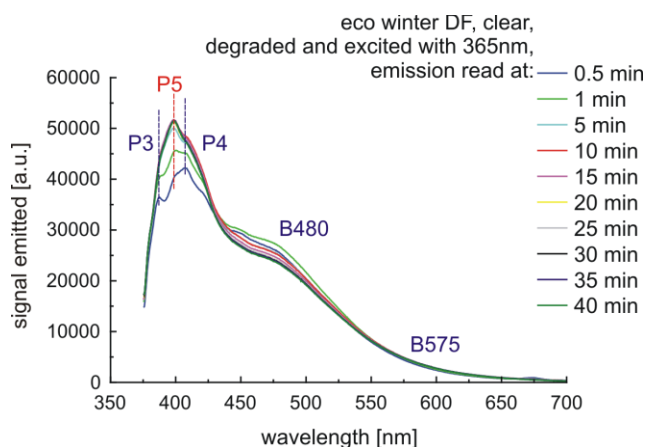


Figure 19. Signal emitted from clear eco winter diesel fuel degraded and excited at 365nm.

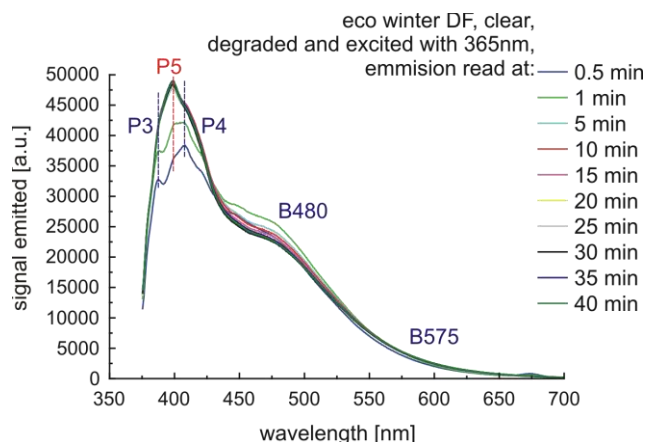


Figure 20. Signal emitted from eco winter diesel fuel with additional improver degraded and excited at 365nm.

The characteristics measured for degradation of eco winter fuel, see Figure 19 and Figure 20, present the new peak (P5) creation as well as P3 and P4 peaks decay.

Besides, the measuring P3 and P4 peaks wavelength shifts seems to be difficult in a sensor device implementation as it requires a spectrometer or a dedicated set of optical filters. But, observation of data gathered in Figures 15-20, leads to the conclusion that amplitude shifts of all mentioned peaks are going in the same direction. Therefore, the wavelength band information (B405) in the range of 380nm to 430nm should illustrate the tendency of signal changes, as presented in Figure 21. In such approximation, the difference between premium and eco type diesel fuel is clear and is the horizontal line at the 30000 [a.u.] of emitted signal.

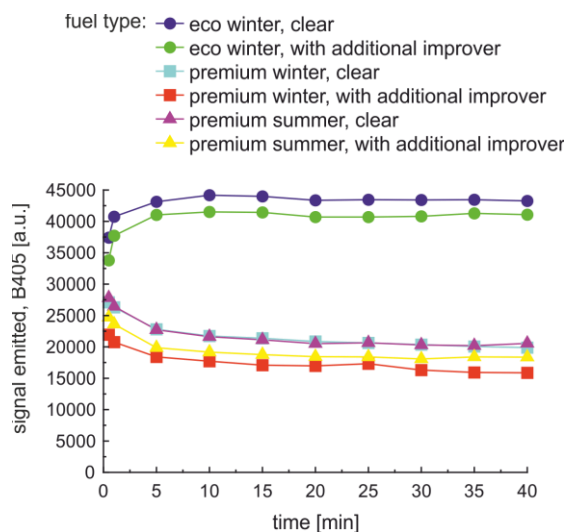


Figure 21. B405 emission in 380nm to 430nm range, excited at 365nm.

The B480 emission for 365 nm excitation seems to be stable, as presented in Figure 22. The most visible changes of signals are for initial period for eco fuel degradation.

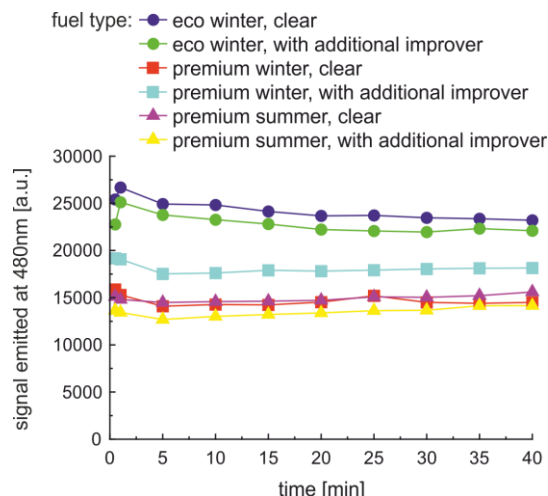


Figure 22. B480 emission excited at 365nm.

Emission at 575 nm, presented in Figure 23, looks different from the characteristic presented in Figure 22. Now, the most stable signals are for eco fuel. But, in both cases the time for saturation may be used as a local fuel stability pointer.

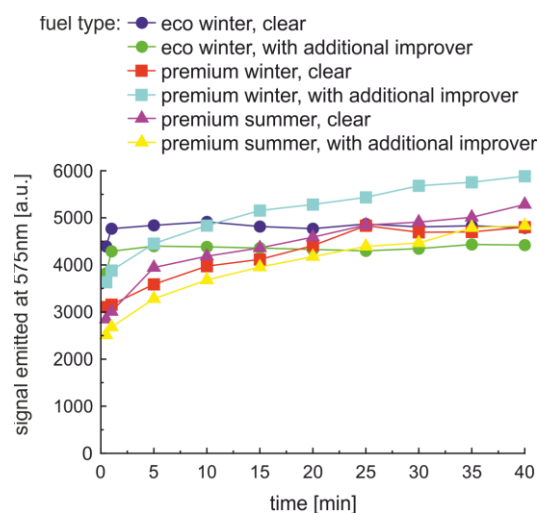


Figure 23. B575 emission excited at 365nm.

The characteristic data points of fuel under with 365 nm radiation degradation, counting from the first minute, are: maximum signal, signal alternation and time to signal saturation at selected wavelength of B405, B480 and B575. They are gathered in Table II.

The most visible aspects here is that the time to saturation that is defined as to the moment when the signal stops to increase, cannot be specified here for some cases. As for example the maximum signal during degradation at 405 nm bandwidth increases only for eco fuel. The maximum signal fuels decreased in 405 nm bandwidth with the use of additional stability improver.

TABLE II. DIESEL FUEL EXAMINATION RESULTS WITH TWO UV SOURCES WORKING AT 365NM

| Fuel type | Maximum signal during degradation [a.u.] | | | Signal alteration [a.u.] | | | Time to saturation [min] | | |
|-----------|--|-------|------|--------------------------|---------------------|---------------------|--------------------------|------|------|
| | B405 | B480 | B575 | B405max -B405min | B480max -B480min | B575max -B575min | B405 | B480 | B575 |
| EWC | 44178 | 26681 | 4914 | 3438 | 3473 | 143 | 10 | - | 10 |
| EWA | 41501 | 25118 | 4435 | 3780 | 3160 | 146 | 10 | - | 5 |
| PWC | 26308 | 19080 | 5885 | 6429 | 1549 | 2003 | - | - | 25 |
| PWA | 20767 | 15297 | 4832 | 4898 | 1201 | 1675 | - | - | 40 |
| PSC | 26437 | 15614 | 5282 | 6250 | 1123 | 2271 | - | - | 40 |
| PSA | 23616 | 14160 | 4832 | 5544 | 1478 | 2152 | - | - | 40 |

As previously (see Table I), the peak signals of eco fuels in B405 bandwidth are greater than for premium fuels. The signals changes suggest an opposite classification of chemical stability than expected, because lower values are observed for eco fuels than premium with except of B480 signal alternation. But, signal alternation is relatively small, calculated in percent versus B405 maximum signal.

IV. CONCLUSIONS

The experiments confirm that fuel fluorescence is a sensitive indicator of photochemical transformations. The UV radiation can be used for fuel sample degradation and fluorescence excitation. The sample irradiation at 265 nm and 365 nm results in different emitted signals changes. The 265 nm irradiation results in amplitude shift of two peaks at 380 nm and 399 nm, and also results in signal development at 480 nm. The sample irradiation at 365 nm results sometimes in the transformation of two peaks to one peak centered at 405 nm. The 405 nm characteristic signal emitted during this examination may be direct related with the generation of benzo[a]pyrene.

Comparing the results gathered in Table I and Table II, we can see that signals variations of P1 and P2 peak registered for degradation with 265 nm wavelength are greater than signal variations of B405 observed for degradation with 365 nm. Therefore, chemical stability of fuel is easier to observation for photo degradation with the use of 265 nm wavelength than with the use of 365 nm. The results of data analysis during fuel irradiation at 265 nm enable to claim, that 40 minutes of UV degradation and sequential fluorescence reading at 10 selected moments of time coupled with data processing is enough to determine the chemical stability of the diesel fuel.

Moreover, the ratio of B405 signals of eco fuels versus premium fuels is about 2:1 for excitation with 365 nm wavelength and is semi-stable during degradation. Therefore, B405 signals can be used to pointing PAHs concentration. In this case, the examination does not have to last more than 15 minutes.

ACKNOWLEDGMENT

This work was supported by the EU Horizon 2020 grant of Teaming for Excellence project ID: 664470, "CEZAMAT-Environment" and by the WUT grant no. 8956/E-365/S/2017, task 504/03115/1035/40.000105.

Authors' contribution: Michał Borecki proposed the method of fuel examination, designed the sensor and analyzed the data from heads and set-ups; Mateusz Gęca proposed the algorithm of time-dependent fuels examination and performed the tests of fuels; Przemysław Prus developed the methods of data processing; Michael L. Korwin-Pawłowski counseled the design process, verified the data analysis and the construction specifications; Jan Szmidi supervised the working plan.

REFERENCES

- [1] M. Borecki, M. Gęca, M. L. Korwin-Pawłowski, and P. Prus, "Capillary sensor with UV-forced degradation and fluorescence reading of diesel and biodiesel fuel chemical stability," The Eighth International Conference on Sensor Device Technologies and Applications (SENSORDEVICES 2017) IARIA, Aug. 2017, pp. 25-30, ISBN: 978-1-61208-581-4.
- [2] J. Bacha et al., Diesel fuels technical review, Chevron Corporation, San Ramon, CA, USA, 2007.
- [3] S. Jain and M. P. Sharma, "Stability of biodiesel and its blends: a review," Renewable and Sustainable Energy Reviews, vol. 14(2), pp. 667-678, 2010.
- [4] C.I.O. Kamalu, A.C. Anarah, A.O. Ogah, P.C. Okere, J.C. Obijaku, F.N. Uzundu, "Kinetic modelling of the combustion of aliphatic hydrocarbons," International Journal of Engineering Research and Allied Sciences, vol. 02, pp. 1-15, 2017.
- [5] D. Patara, K.L. Sireesha, A.K. Mishra, "Determination of synchronous fluorescence scan parameters for certain petroleum products," Journal of Scientific & Industrial Research, vol. 59, pp. 300-305, 2000.
- [6] B. L. Smith, L. S. Ott, and Thomas J. Bruno, "Composition-explicit distillation curves of commercial biodiesel fuels:

- comparison of petroleum-derived fuel with B20 and B100," *Ind. Eng. Chem. Res.*, vol. 47, pp. 5832-5840, 2008.
- [7] M. G. Fonseca et al., "Advanced techniques in soybean biodiesel," H. El-Shemy (Ed.), *Soybean - Bio-Active Compounds*, InTech, Rijeka, Croatia, 2013.
- [8] R. A. Korus, T. L. Mousetis, and L. Lloyd, "Polymerization of vegetable oils," *American Society of Agricultural Engineering*, vol. 4, pp. 127-137, 1982.
- [9] Technical Committee of Petroleum Additive Manufactures in Europe, "Fuel additives: use and benefits," ATC Document, vol. 113, pp. 1-68, 2013.
- [10] C.C. Gaylarde, F.M. Bento, and J. Kelly, "Microbial contamination of stored hydrocarbon fuels and its control," *Rev. Microbiol.*, vol. 30, pp. 1-10, 1999.
- [11] L. F. Bautista, C. Vargas, N. González, M. C. Molina, R. Simarro, A. Salmerón, and Y. Murillo, "Assessment of biocides and ultrasound treatment to avoid bacterial growth in diesel fuel," *Fuel Processing Technology*, vol. 152, pp. 56-63, 2016.
- [12] D. E. Nicodem, C. L. B. Guedes, R. J. Correa, and M. C. Z. Fernandes, "Photochemical processes and the environmental impact of petroleum spills," *Biogeochemistry*, vol. 39(2), pp. 121-138, 1997.
- [13] D. L. Plata, C. M. Sharpless, and C. M. Reddy, "Photochemical degradation of polycyclic aromatic hydrocarbons in oil films," *Environmental Science and Technology*, vol. 42(7), pp. 2432-2438, 2008.
- [14] A. Dwivedi, A. Kumar, and J.L. Bhat, "Effect of UV radiation on the growth and petroleum hydrocarbon degradation ability of bacteria," *Oct. Jour. Env. Res.*, vol. 5(1), pp. 032-040, 2017.
- [15] R. Lin and L.L. Tavlarides, "Thermal stability and decomposition of diesel fuel under subcritical and supercritical conditions," *Journal of Supercritical Fluids*, vol. 75, pp. 101-111, 2013.
- [16] J. Czarnocka and M. Odziemkowska, "Diesel fuel degradation during storage process," *Chemik*, vol. 69, pp. 771-776, 2015.
- [17] J.P. Wan, "Properties of fats and oils," in *Introduction to Fat and Oils Technology*, AOCS Press, Champaign Illinois, pp. 20-49, 2000.
- [18] L. Zhang, P. Li, Z. Gong, and X. Li, "Photocatalytic degradation of polycyclic aromatic hydrocarbons on soil surfaces using TiO₂ under UV light," *Journal of Hazardous Materials*, vol. 158, pp. 478-484, 2008.
- [19] O. T. Woo, W. K. Chung, K. H. Wong, A. T. Chow, and P. K. Wong, "Photocatalytic oxidation of polycyclic aromatic hydrocarbons: Intermediates identification and toxicity testing," *Journal of Hazardous Materials*, vol. 168, pp. 1192-1199, 2009.
- [20] M. Nandi and D. Jacobs, "Cetane response of di-tertiary-butyl peroxide in different diesel fuels," *SAE Technical Paper*, vol. 952368, pp. 952368:1-18, 1995.
- [21] H. O. Pritchard and P. Q. E. Clothier, "Anaerobic operation of an internal combustion engine," *J. Chem. Soc. Chem. Commun.*, vol. 20, pp. 1529-1530, 1986.
- [22] 2EHN Industry Work Group, "2-Ethylhexyl nitrate (2EHN) best practices manual," ATC, doc. 79, pp. 1-24, 2004.
- [23] H. Bornemann, F. Scheidt, and W. Sander, "Thermal Decomposition of 2-Ethylhexyl Nitrate (2-EHN)," *Int. J. of Chemical Kinetics*, vol. 34, pp. 34-38, 2002.
- [24] M. Insausti and B. S. Fernández-Band, "Determination of 2-ethylhexyl nitrate in diesel oil using a single excitation emission fluorescence spectra (EEF) and chemometrics analysis," *J. Fundamentals of Renewable Energy and Applications*, vol. 4, pp. 1000137:1-4, 2014.
- [25] C. Schaschke, I. Fletcher, and N. Glen, "Density and Viscosity Measurement of Diesel Fuels at Combined High Pressure and Elevated Temperature," *Processes*, vol. 1, pp. 30-48, 2013.
- [26] G. Fannin, "Distillation process analyser with ASTM D86 Compliance," *Petro Industry News*, no. August/September, pp. 40-41, 2013.
- [27] P. J. García Moreno, R. Perez-Galvez, A. Guadix, and E. M. Guadix, "Influence of the parameters of the Rancimat test on the determination of the oxidative stability index of cod liver oil," *L W T- Food Science and Technology*, vol. 51, pp. 303-308, 2013.
- [28] J. H. Hildebrand, "Factors Determining Chemical Stability," *Chem. Rev.*, vol. 2, pp. 395-417, 1926.
- [29] R. T. Jarviste, R. T. Muoni, J. H. Soone, H. J. Riisalu, and A. L. Zaidentsal, "Diesel fuel oxidation in storage," *Solid Fuel Chemistry*, vol. 42, pp. 123-127, 2008.
- [30] D. Patra and A. K. Mishra, "Study of diesel fuel contamination by excitation emission matrix spectral subtraction fluorescence," *Analytica Chimica Acta*, vol. 454, pp. 209-215, 2002.
- [31] Marilena Meira et al., "Determination of Adulterants in Diesel by Integration of LED Fluorescence Spectra," *J. Braz. Chem. Soc.*, vol. 26, pp. 1351-1356, 2015.
- [32] M. Włodarski, A. Bombalska, M. Mularczyk-Oliwa, M. Kaliszewski, and K. Kopczyński, "Fluorimetric techniques in analysis and classification of fuels," *Proc. SPIE 8703*, pp. 87030B:1-7, 2013, DOI: 10.1117/12.2011706.
- [33] M. Rasouli, S. H. Tavassoli, S. J. Mousavi, and S. M. R. Darbani, "Measuring of naphthalene fluorescence emission in the water with nanosecond time delay laser induced fluorescence spectroscopy method," *Optik*, vol. 127, pp. 6218-6223, 2016.
- [34] S. Chikh, Y.B. Pemanos, T. Zourane, and B. Hamada, "Synthesis of a biobased antioxidant additive for diesel fuel," *American Journal of Applied Chemistry*, vol. 2(1), pp. 10-14, 2014.
- [35] C. L. B. Guedes, E. DiMauro, A. De Campos, L. F. Mazzochin, G. M. Bragagnolo, F. A. De Melo, and M. T. Piccinato, "EPR and fluorescence spectroscopy in the photodegradation study of arabian and colombian crude oils," *International Journal of Photoenergy*, vol. 2006, pp. 48462:1-6, 2006, DOI 10.1155/IJP/2006/48462.
- [36] M. Borecki et al., "Fiber optic capillary sensor with smart optode for rapid testing of the quality of diesel and biodiesel fuel," *IJASM*, vol. 7, pp. 57-67, 2014.
- [37] M. Borecki et al., "Dynamical capillary rise photonic sensor for testing of diesel and biodiesel fuel," *Sensors & Transducers Journal*, vol. 193, pp. 11-22, 2015.
- [38] M. Borecki and M.L. Korwin-Pawlowski, "Capillary sensor with UV-VIS reading of effects of diesel and biodiesel fuel degradation in storage," *Sensors & Transducers*, vol. 205, pp. 1-9, 2016.
- [39] A. Baranowska, P. Miluski, M. Kochanowicz, J. Zmojda, and D. Dorosz, "Capillary optical fibre with Sm³⁺ doped ribbon core," *Proc. SPIE*, vol. 9662, pp. 96620Z, 2015.
- [40] M. Geca, M. Borecki, M. L. Korwin-Pawlowski, and A. Kociubiński, "Local liquid sample heating: integration and isolation of a micro-heater," *Proc. SPIE*, vol. 9662, pp. 96620E, 2015.
- [41] A. Kociubiński, M. Borecki, M. Duk, M. Sochacki, and M. L. Korwin-Pawlowski, "3D photodetecting structure with adjustable sensitivity ratio in UV-VIS range," *Microelectronic Engineering*, vol. 154, pp. 48-52, 2016.
- [42] P. Doroz, M. Duk, M. L. Korwin-Pawlowski, and M. Borecki, "Amplifiers dedicated for large area SiC photodiodes," *Proc SPIE*, vol. 10031, pp. 100311R, 2016.

- [43] P. Prus, M. Borecki, M. L. Korwin-Pawłowski, A. Kociubiński, and M. Duk, "Automatic detection of characteristic points and form of optical signals in multiparametric capillary sensors," *Proc. SPIE*, vol. 9290, pp. 929009, 2014.
- [44] M. T. Ibrahim, R. Telford, P. Dini, P. Lorenz, N. Vidovic, and R. Anthony, "Self-adaptability and man-in-the-loop: a dilemma in autonomic computing systems," *Proc. IEEE Computer Society 15th International Workshop on Database and Expert Systems Applications*, Los Alamitos, California, USA, pp. 722-729, 2004.
- [45] V. Zamora, Z. Zhang and A. Meldrum, "Refractometric Sensing of Heavy Oils in Fluorescent Core Microcapillaries," *Oil & Gas Science and Technology – Rev. IFP Energies nouvelles*, vol. 70(3), pp. 487-495, 2015.
- [46] S. Y. Yurish, N. V. Kirianaki, and R. Pallàs - Areny, "Universal frequency - to - digital converter for quasi - digital and smart sensors: specifications and applications," *Sensor Review*, vol. 25(2), pp. 92-99, 2005.
- [47] Z. Bielecki, "Readout electronics for optical detectors," *Optoelectronics Review*, vol. 12, pp. 129-137, 2004.
- [48] P. Firek, A. Werbowy, and J. Szmids, "MIS field effect transistor with barium titanate thin film as a gate insulator," *Materials Science and Engineering B: Solid-State Materials for Advanced Technology*, vol. 165(1-2), pp. 126-128, 2009.
- [49] R. Srinivasan, "Photochemistry of conjugated dienes and trienes," in *Advances in Photochemistry*, vol. 4, Eds. W. A. Noyes, G. S. Hammond and J. N. Pitts, John Wiley & Sons, Hoboken, NJ, USA, 1966.
- [50] C.M. Carruco Laranjeira et al., "Used food oils: physical-chemical indicators of quality degradation," *Proc. FOODBALT 2017*, pp. 154-159, 2017. DOI: 10.22616/foodbalt.2017.040.
- [51] A. M. Rivera-Figueroa, K. A. Ramazan, and B. J. Finlayson-Pitts, "Fluorescence, absorption, and excitation spectra of polycyclic aromatic hydrocarbons as a tool for quantitative analysis," *J. of Chemical Education*, vol. 81, pp. 242-245, 2004.
- [52] C. Brussol, M. Duane, P. Carlier, and D. Kotzias, "Photo-induced OH reactions of naphthalene and its oxidation products on SiO₂," *Environ. Sci. Pollut. Res. Int.*, vol. 6(3), pp. 138-140, 1999.
- [53] S. Hachiya, K. Asai, and G.-i. Konishi, "Unique solvent-dependent fluorescence of nitro-group-containing naphthalene derivatives with weak donor-strong acceptor system," *Tetrahedron Letters*, vol. 54, pp. 1839-1841, 2013.
- [54] L. H. Zhang, C.B. Xu, Z. L. C, and X. M. Li, "Effect of UV Intensity and Wavelength on Photocatalytic Degradation of Polycyclic Aromatic Hydrocarbons," *Advanced Materials Research*, vols. 233-235, pp. 466-469, 2011.
- [55] F. Valerio and A. Lazzarotto, "Photochemical Degradation of Polycyclic Aromatic Hydrocarbons (PAH) in Real and Laboratory Conditions," *International Journal of Environmental Analytical Chemistry*, vol. 23, pp. 135-151, 1985.
- [56] S. Bertilsson and A. Widenfalk, "Photochemical degradation of PAHs in freshwaters and their impact on bacterial growth – influence of water chemistry," *Hydrobiologia* vol. 469, pp. 23–32, 2002.
- [57] D. E. Nicodem, C. L. B. Guedes, and R. J. Correa, "Photochemistry of petroleum I. Systematic study of a Brazilian intermediate crude oil," *Marine Chemistry*, vol. 63, pp. 93-104, 1998.
- [58] I. Beriman, "Handbook of fluorescence spectra of Aromatic Molecules –2nd Edition" Academic Press, New York, 1971.